Title

Two tonoplast MATE proteins function as turgor-regulating chloride channels in Arabidopsis

Journal

Proceedings of the National Academy of Sciences of the United States of America, 114(10)

ISSN

0027-8424

Authors

Zhang, Haiwen
Zhao, Fu-Geng
Tang, Ren-Jie
et al.

Publication Date

2017-03-07

DOI

10.1073/pnas.1616203114

Peer reviewed

Two tonoplast MATE proteins function as turgor-regulating chloride channels in *Arabidopsis*

Haiwen Zhang[a,b,c,d], Fu-Geng Zhao[a,1], Ren-Jie Tang[c], Yuexuan Yu[b], Jiali Song[b], Yuan Wang[a], Legong Li[b,1], and Sheng Luan[c,1]

[a]Institute of Plant Molecular Biology, State Key Laboratory of Pharmaceutical Technology, School of Life Sciences, Nanjing University, Nanjing 210093, China; [b]College of Life Sciences, Capital Normal University, Beijing 100048, China; [c]Department of Plant and Microbial Biology, University of California, Berkeley, CA 94720; and [d]Beijing Key Laboratory of Agricultural Genetic Resources and Biotechnology, Beijing Agro-Biotechnology Research Center, Beijing Academy of Agriculture and Forestry Sciences, Beijing 100097, China

Edited by Natasha V. Raikhel, Center for Plant Cell Biology, Riverside, CA, and approved December 15, 2016 (received for review October 7, 2016)

The central vacuole in a plant cell occupies the majority of the cellular volume and plays a key role in turgor regulation. The vacuolar membrane (tonoplast) contains a large number of transporters that mediate fluxes of solutes and water, thereby adjusting cell turgor in response to developmental and environmental signals. We report that two tonoplast Detoxification efflux carrier (DTX)/Multidrug and Toxic Compound Extrusion (MATE) transporters, DTX33 and DTX35, function as chloride channels essential for turgor regulation in *Arabidopsis*. Ectopic expression of each transporter in *Nicotiana benthamiana* mesophyll cells elicited a large voltage-dependent inward chloride current across the tonoplast, showing that DTX33 and DTX35 each constitute a functional channel. Both channels are highly expressed in *Arabidopsis* tissues, including root hairs and guard cells that experience rapid turgor changes during root-hair elongation and stomatal movements. Disruption of these two genes, either in single or double mutants, resulted in shorter root hairs and smaller stomatal aperture, with double mutants showing more severe defects, suggesting that these two channels function additively to facilitate anion influx into the vacuole during cell expansion. In addition, *dtx35* single mutant showed lower fertility as a result of a defect in pollen-tube growth. Indeed, patch-clamp recording of isolated vacuoles indicated that the inward chloride channel activity across the tonoplast was impaired in the double mutant. Because MATE proteins are widely known transporters of organic compounds, finding MATE members as chloride channels expands the functional definition of this large family of transporters.

vacuole | root hair | stomata | drought

Within a plant cell, turgor pressure pushes the plasma membrane against the cell wall to generate a specific cell size and shape (1–3). Hence, turgor pressure is the driving force for cell expansion and growth. At the tissue level, the structural strength of tissues depends on both the cell wall rigidity and turgor pressure in each cell. The tissues remain turgid when turgor pressure rises and wilt when turgor falls below a certain threshold (2–4). Therefore, turgor is essential for cell growth and morphology, tissue architecture, and overall strength of all plants.

Positive turgor pressure is produced when osmolality of intracellular content is higher than the extracellular environment (apoplast), leading to water intake and cell swelling. Because most living plant cells contain a large central vacuole that can occupy as much as 90% of the cellular volume, vacuolar lumen provides the major space for turgor regulation. Vacuoles also function as a depository of xenobiotic and toxic compounds, minimizing toxicity in the cytoplasm where sensitive biochemical processes take place. Secondary metabolites and proteins involved in plant defense against pathogens and herbivores are also kept in the vacuole and released in response to attack and cellular damage (5). Vacuoles play a critical role in pH regulation as well, with its own pH typically around 5–6 because of action of H^+-ATPases and pyrophosphatase that pump protons into the lumen (6). In all cases, the tonoplast transport proteins are key players that enable these functions. For example, the tonoplast ATP binding cassette transporters are responsible for detoxifying many secondary compounds from the cytoplasm (7, 8). The chloride channel (CLC)–type ion channels play a role in sequestration of anions, including nitrate and chloride, into the vacuole (9). Some cation channels and transporters have also been shown to be present and in charge of cation fluxes in and out of vacuoles (10–13). Last but not least, aquaporins represent the most abundant tonoplast proteins that move water across the vacuolar membrane to adjust turgor pressure (14).

The Detoxification efflux carrier (DTX)/Multidrug and Toxic Compound Extrusion (MATE) transporters are conserved from bacteria to plants and animals (15). Consistent with the diversity of secondary metabolites in plants, a large and diverse family of DTX/MATE proteins has been identified in plant genomes. The *Arabidopsis* genome encodes at least 56 members in the DTX/MATE family (16), among which several members have been reported to function as transporters of organic acids and secondary metabolites. For example, AtDTX1 serves as an efflux carrier of plant-derived alkaloids and antibiotics (16). The TT12 protein works as a flavonoid/H^+ antiporter in seed coat cells (17). The FRD3 protein is a citric acid efflux transporter involved in effective Fe^{3+} uptake (18). The EDS5 protein plays a role in the salicylic acid (SA)-dependent pathogen response pathway and possibly functions as an SA transporter responsible for SA release from chloroplasts (19, 20). Our previous work indicates that AtDTX50 may serve as an abscisic acid (ABA) efflux transporter (21). A

Significance

Turgor pressure is the driving force for cell growth in plants, and the large central vacuole provides the major space for turgor regulation. However, the molecular identity and function of many transporters that control water and solute fluxes in and out of vacuoles remain unknown. We report here that two Multidrug and Toxic Compound Extrusion (MATE)-type transporters show previously unrecognized function as chloride channels essential for turgor regulation in *Arabidopsis*. The MATE transporters are highly conserved from bacteria, fungi, plants, to animals, and widely accepted as transporters of organic compounds. This study, showing some MATE transporters as chloride channels, thus breaks the old dogma on the functional definition of this large family of transporters.

Author contributions: H.Z., F.-G.Z., L.L., and S.L. designed research; H.Z., F.-G.Z., Y.Y., J.S., and Y.W. performed research; R.-J.T. and Y.W. contributed new reagents/analytic tools; H.Z., F.-G.Z., L.L., and S.L. analyzed data; and H.Z., F.-G.Z., L.L., and S.L. wrote the paper.

The authors declare no conflict of interest.

This article is a PNAS Direct Submission.

Freely available online through the PNAS open access option.

[1]To whom correspondence may be addressed. Email: fgzhao@nju.edu.cn, lgli@cnu.edu.cn, or sluan@berkeley.edu.

This article contains supporting information online at www.pnas.org/lookup/suppl/doi:10.1073/pnas.1616203114/-/DCSupplemental.

recent study indicates that DTX18 exports hydroxycinnamic acid amides to the leaf surface, inhibiting germination of *Phytophthora infestans* spores (22).

To explore the functional diversity of the large DTX/MATE transporter family in plants and in particular, those in the vacuolar membrane, we focus here on the characterization of two closely related members, DTX33 and DTX35, which are localized to the tonoplast. Surprisingly, these two members, unlike those reported previously, function as typical anion channels that transport inorganic anions, especially chloride. We further identified their function as influx channels that facilitate chloride sequestration into the vacuole. Genetic mutant analyses linked their function to root-hair growth and stomatal movement in *Arabidopsis*.

Results

DTX33 and DTX35 Are Highly Similar Proteins Localized to the Tonoplast, and Their Genes Are Widely Expressed in *Arabidopsis* Tissues. Since the identification of AtDTX1 by bacterial complementation (16), we have started a systematic analysis of functional redundancy of these DTX/MATE family transporters. We approached their functional relatedness based on their phylogenetic relations, expression patterns, and subcellular locations. One proteomic study (23) identified six DTX proteins associated with the tonoplast. In the phylogenetic tree, two of the members are closely related and named as DTX33 and DTX35. We focused on these two members and examined their functional relationship.

Because subcellular localization of a transporter is critical for its function, we first examined their subcellular localization by the GFP fusion approach to corroborate the proteomics results. We made *DTX33::GFP* and *DTX35::GFP* fusion constructs under the control of 35S promoter and transiently expressed them in *Arabidopsis* suspension culture cells (24). Because these cells lack chloroplasts, the plasma membrane and vacuolar membrane were often separated by asymmetrical distribution of the cytoplasm. The DTX33-GFP and DTX35-GFP were clearly associated with the vacuolar membrane as was AtTPK1-GFP, a well-known tonoplast protein (25) (Fig. 1*A*). In the transgenic plants expressing the DTX33-GFP or DTX35-GFP, we found that the green fluorescence was particularly strong in stomatal guard cells, although the 35S promoter was not supposed to drive specific expression of the fusion protein. Nevertheless, guard cell provided a model cell to examine the subcellular localization of the fusion proteins. We found that DTX33-GFP and DTX35-GFP were associated with guard cell periphery that was separated from plasma membrane stained with FRIE MAO 4-64 (FM4-64) dye (Fig. 1*B* and Fig. S1). We further confirmed the tonoplast localization by examining the fluorescence signals on vacuoles released from *Arabidopsis* mesophyll protoplasts transfected by the DTX-GFP constructs. The released vacuoles after osmotic breakage of plasma membrane are still associated with chloroplast clusters on the outside (shown by red autofluorescence from chlorophyll) (Fig. 1*C*). Together, these results confirmed the previously reported proteomic data that both DTX33 and DTX35 are tonoplast proteins.

Another important feature that determines a gene function is its expression pattern. To investigate the expression patterns of the two genes encoding DTX33 and DTX35, we performed real-time PCR assay and found that mRNA levels of both genes are quite high in various tissues, including roots, leaves, and flowers, suggesting that both genes are ubiquitously expressed in a plant (Fig. 2 *A* and *B*). To assess the expression of these genes in more detail, we fused their promoter regions (2.0 kb upstream of the start codon) to the β-glucuronidase (GUS) reporter and transformed the constructs into *Arabidopsis*. We found that GUS activities driven by both gene promoters were detected in a variety of plant tissues, including roots, mesophyll cells, guard cells, inflorescence stems, and flowers (Fig. 2 *C* and *D*). Furthermore, the overall expression pattern of *DTX33* and *DTX35* was highly similar, suggesting possible overlap of functions.

Expression of DTX33 or DTX35 in *Nicotiana benthamiana* Elicits a Large Voltage-Dependent Chloride Current Across Tonoplast. Because DTX family proteins are transporters with a variety of substrates, their physiological functions are tied to their transport properties. To address the transport activity and substrate specificity of DTX33 and DTX35, we need to express these transporters in plant cells where the proteins are targeted to the

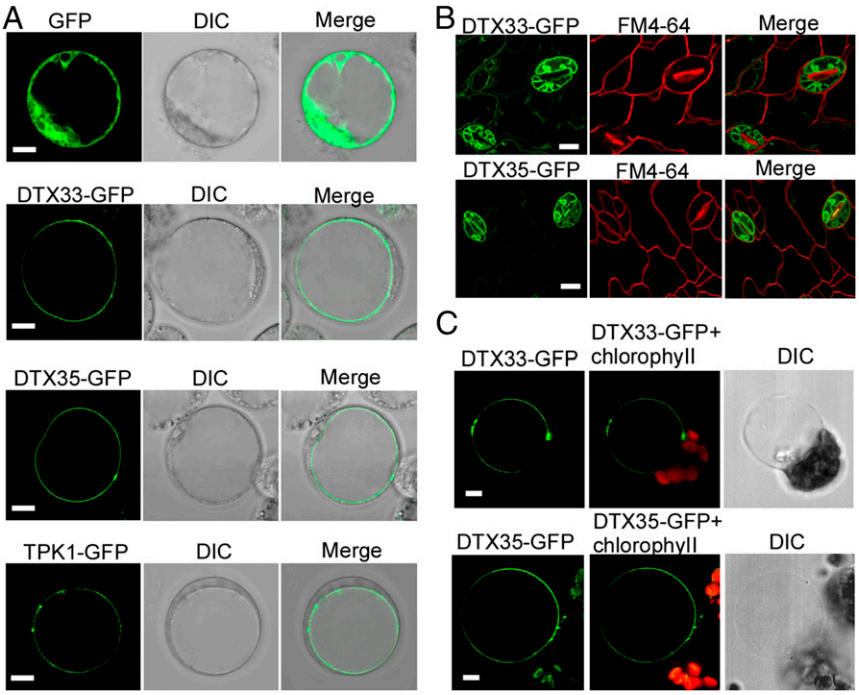

Fig. 1. DTX33 and DTX35 are both tonoplast proteins. (*A*) *Arabidopsis* suspension culture cells were transiently transformed with *35S-DTX33::GFP*, *35S-DTX35::GFP*, or *35S-TPK1::GFP*. (*Left*) GFP signals (green), (*Center*) bight field image of the same cell (DIC), and (*Right*) an overlay (GFP and DIC) of the same sample. (Scale bar: 5 μM.) (*B*) Transgenic *Arabidopsis* plants expressing *35S:DTX33-GFP* and *35S:DTX35-GFP*. (*Left*) GFP signals (green), (*Center*) the plasma membrane stained with FM4-64 (red), and (*Right*) an overlay (green and red) from the same sample. (Scale bar: 20 μM.) (*C*) Vacuoles released from *Arabidopsis* mesophyll protoplasts that were transiently transformed with *35S-DTX33::GFP* and *35S-DTX35::GFP*. (Scale bar: 5 μM.)

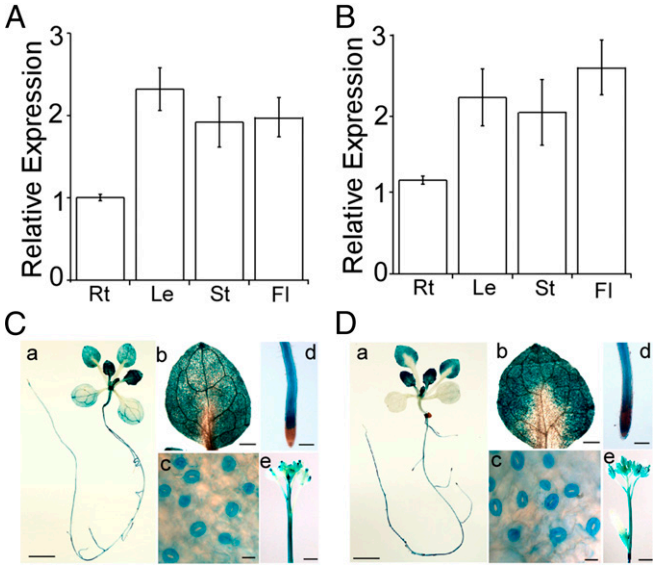

Fig. 2. Expression patterns of *DTX33* and *DTX35*. (*A* and *B*) Real-time PCR analysis of mRNA levels of *DTX33* and *DTX35* in different tissues. Data represent mean ± SD. Fl, flower; Le, leaf; Rt, root; St, stem. (*C*) Expression pattern of *DTX33-GUS* showing (*a*) 2-wk-old plant, (*b*) leaf, (*c*) guard cells, (*d*) root, and (*e*) flower. (Scale bar: *a* and *e*, 5 mm; *b* and *d*, 0.5 mm; *c*, 50 μm.) (*D*) Expression pattern of *DTX35-GUS* showing (*a*) 2-wk-old plant, (*b*) leaf, (*c*) guard cells, (*d*) root, and (*e*) flower. (Scale bar: *a* and *e*, 5 mm; *b* and *d*, 0.5 mm; *c*, 50 μm.)

vacuolar membrane so that their in situ activity can be measured. Previous studies (26, 27) used agrobacterium-mediated transformation of *Nicotiana benthamiana* mesophyll cells as a functional expression system for vacuolar transporters. Although the vacuoles isolated from these cells display endogenous transport activity, overexpression of an exogenous transporter drives the transport activity many folds over the background, thus making it feasible to analyze the function and characteristics of the exogenous vacuolar transporters (28). To monitor the expression of *DTX33* or *DTX35*, we expressed the proteins as GFP fusions in *N. benthamiana* mesophyll cells. We then measured the transport activity of isolated vacuoles from fluorescence-labeled cells by patch-clamp procedure (28). Several studies indicated that DTX/MATE-type proteins transport organic acids, such as citric acid (18–22, 29). We examined the possibility that DTX33 and DTX35 may function as anion transporters, like those reported earlier. We performed the patch-clamp procedure under a whole-vacuole configuration in bath solutions containing cation BisTrisPropane (BTP) and various anions, including citric acid, malate, chloride, nitrate, phosphate, sulfate, bromide, and glutamate. BTP is generally impermeable, thus minimizing the contribution of cation current (30). As documented previously, an "inward" current is defined as movement of a positive charge out of or a negative charge into the vacuole (31). We compared the current amplitudes produced by various anions and found that chloride consistently generated a large voltage-dependent inward current. Compared with the endogenous background expressing the empty vector, increases in Cl^- current densities at −160 mV were 4.4- and 5.1-fold for vacuoles overexpressing *DTX33-GFP* and *DTX35-GFP*, respectively (empty vector: 2.6 ± 0.3 pA·pF^{-1}, $n = 11$; *DTX33-GFP*: 11.5 ± 0.6 pA·pF^{-1}, $n = 7$; *DTX35-GFP*: 13.2 ± 0.7 pA·pF^{-1}, $n = 6$) (Fig. 3 *A*–*C*). To further address the anion selectivity of the currents observed in vacuoles containing *DTX33-GFP* and *DTX35-GFP*, we performed a rapid voltage ramp analysis (50 mV·s^{-1})to directly measure the reversal potentials of the currents. Replacing 100-mM Cl^- bath solution with different equimolar anions resulted in significant shifts of the reversal potentials (Fig. S2). On the basis of reversal potentials, the following relative permeability sequence was derived (30): for DTX33, Br^- (17.5 ± 2.0 mV) > Cl^- (−2.2 ± 0.8 mV) > NO_3^- (−12.5 ± 0.9 mV) ~ malate^{2-} (−11.6 ± 1.3 mV) > citrate^{3-} (−17 ± 2.0 mV) > HPO_4^{2-} (−34 ± 2.5 mV) ~ SO_4^{2-} (−36 ± 2.8 mV) > glutamate^{2-} (−71 ± 2 mV); for DTX35, Br^- (11.5 ± 1.0 mV) > Cl^- (−3.2 ± 0.9 mV) > NO_3^- (−9.5 ± 0.8 mV) ~ malate^{2-} (−12.6 ± 1.5 mV) ~ citrate^{3-} (−13.1 ± 2.0 mV) > HPO_4^{2-} (−33 ± 2.6 mV) ~ SO_4^{2-} (−37 ± 1.8 mV) > glutamate^{2-} (−56 ± 2.1 mV) (Fig. 3 *D* and *E* and Table S1). To study the possible effect of anions in the vacuolar lumen on the channel current, we substituted the vacuolar chloride with equal amounts of malate and nitrate and found that the amplitudes of inward Cl^- currents did not change significantly (Fig. S3). To exclude the possibility that DTX33 and DTX35 may function as a cation transporter, thereby generating the channel currents observed, we measured the potassium currents across the vacuolar membrane using the *N. benthamiana* system transformed with *DTX33-GFP* or *DTX35-GFP*. We found that the outward K^+ currents (that could contribute to the anion influx currents) observed in vacuoles expressing DTX33-GFP or DTX35-GFP were not significantly different from the vector control (Fig. S4). In conclusion, considering that most land plants do not use bromide as a functional anion, the results from the above analyses indicate that DTX33 and DTX35 exhibited highest selectivity for Cl^- over other anions in plants (Fig. 3 *D* and *E*). The DTX33 and DTX35 transporters were not significantly permeable to organic acids, including citric acid and malate, in contrast to the MATE transporters described previously, including those mediating aluminum tolerance (18–22, 29). It is noteworthy that both DTX members are slightly permeable to nitrate, which can be an abundant inorganic anion in plant cells under certain soil conditions. It is, therefore, possible that nitrate transport through these MATE proteins can be physiologically relevant in the context of turgor regulation.

To investigate further the transport properties of DTX33 and DTX35, we included various concentrations of Cl^- in the bath solution and found that DTX33- and DTX35-mediated currents were highly dependent on cytosolic Cl^- concentration (Fig. 4 *A*, *B*, *D*, and *E* and Fig. S5). When cytosolic Cl^- (as represented by bath Cl^-) reached a level symmetrical to that in the vacuolar lumen (100 mM Cl^-_{cyt}/100 mM Cl^-_{vac}), the current amplitudes of *DTX33-GFP*– and *DTX35-GFP*–expressing vacuoles were increased by 14- and 16-fold, respectively, compared with the current recorded under 1 mM Cl^-_{cyt}/100 mM Cl^-_{vac} condition (Fig. 4 *A*, *B*, *D*, and *E*). The reversal potentials (E_{rev}) of DTX33 and DTX35 currents shifted to more positive values with increasing cytosolic Cl^- concentrations, which correlated well with the Nernst prediction of Cl^- equilibrium potentials (Fig. 4 *C* and *F*, Fig. S5, and Table S2). The agreement between measured and predicted Nernst potentials for Cl^- showed that DTX33 and DTX35 behave as ion channels, mediating the passive transport of Cl^- across the vacuolar membrane.

We also analyzed the single-channel activities in membrane patches detached from vacuoles isolated from *N. benthamiana* mesophyll cells transformed with empty vector (control), *35S:DTX33-GFP*, or *35S:DTX35-GFP* construct. Single-channel activity was not detected in the patches from control vacuoles under Cl^--based bath and pipette solutions ($n = 10$). In contrast, we consistently recorded single-channel conductance in all excised outside-out patches from vacuoles overexpressing *DTX33-GFP* or *DTX35-GFP* ($n = 12$ for each construct). The single-channel open probability (Po) of DTX33 or DTX35 depended on voltage and increased at more negative membrane potentials (Fig. 5 *A* and *B*), which is in agreement with the whole-vacuole measurements (Fig. 3*A*). As the membrane potential shifted from −40 to −120 mV, the Po values of DTX33 and DTX35 increased 10- and 7-fold, respectively (Fig. 5 *A* and *B*). The single-channel current amplitudes also increased with more negative

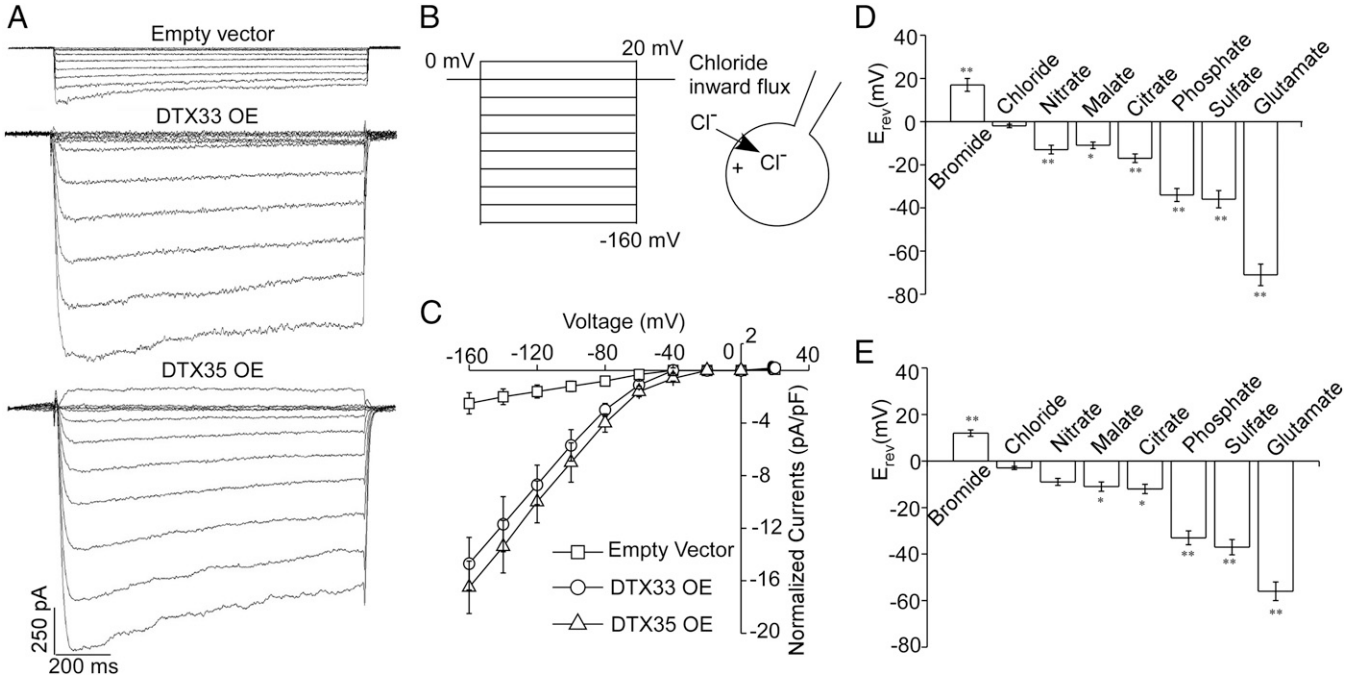

Fig. 3. DTX33 and DTX35 mediate chloride transport across the vacuolar membrane. (*A*) Representative whole-vacuole current of vacuoles isolated from *N. benthamiana* mesophyll cells transformed by empty vector, *DTX33-GFP*, or *DTX35-GFP*. OE, over expression cell. (*B*) Recording protocol. From a holding potential of 0 mV, a series of test voltages from −160 to 20 mV in steps of 20 mV was applied. Symmetrical chloride levels (100 mM Cl^-_{cyt}/100 mM Cl^-_{vac}) were used in all recordings. (*C*) Current–voltage relationships from vacuoles as in *A* for vector control ($n = 13$), DTX33-GFP ($n = 8$), and DTX35-GFP ($n = 7$). Steady-state currents were determined by averaging the first 50–100 ms of each current trace. The data represent mean ± SD. (*D* and *E*) Bar plots of reversal potentials illustrating anion selectivity. The vacuolar side contains 100 mM Cl^-, and a cytosolic solution contains 100 mM different anions (chloride, bromide, nitrate, malate, citrate, phosphate, sulfate, or glutamate). Data are means ± SEM, and one-way ANOVA analysis was used to identify significant differences at the $P < 0.05$ or 0.01 level. $*P < 0.05$; $**P < 0.01$.

tonoplast potentials, with 50- and 80-pS conductance, respectively, at −120 mV (Fig. 5 *A* and *B*). The reversal potentials of the single channels were −2 ± 2 and 0 ± 2 mV, respectively, in agreement with the Nernst potential for Cl^- [$E_{Nernst}(Cl^-) = 0$ mV] (Fig. 5 *C* and *D*).

Disruption of DTX33 and DTX35 Expression Reduces Vacuolar Chloride Influx. If *DTX33* and *DTX35* function as CLCs mediating chloride influx into the vacuolar lumen, disruption of these two genes should reduce the chloride influx and thus, alter cell turgor regulation and related physiological processes. To test this hypothesis, we identified two transfer-DNA (T-DNA) insertional mutant alleles for *DTX33* (*dtx33-1* and *dtx33-2*) and one allele for *DTX35* (*dtx35*). After obtaining homozygous mutants, we examined the transcript levels of these two genes and found that all three mutants represented null alleles lacking a detectable level of mRNA. Two double mutants, *dtx33-1*/*dtx35* and *dtx33-2*/*dtx35*, were obtained after crossing the single mutants, and they lacked both *DTX33* and *DTX35* mRNA (Fig. 6 *A* and *B*).

To record channel activity across *Arabidopsis* vacuolar membrane, we performed the patch-clamp procedure on isolated vacuoles from mesophyll cells of the WT, *dtx33-1*, *dtx33-2*, *dtx35*, *dtx33-1*/*dtx35*, and *dtx-2*/*dtx35* mutants. We conducted the experiments using the same buffer (100 mM Cl^-_{cyt}/100 mM Cl^-_{vac}) and the same protocol (−160 to +20 mV) as in the experiments with *N. benthamiana* vacuoles. In the whole-vacuole recording from the WT plants, a chloride current was observed. The inward rectifying chloride current depended on negative voltage (Fig. 6*C*). The mean current density at −160 mV was −3 pA/pF (Fig. 6*D*). We performed the same experiments in *dtx33-1*, *dtx33-2*, *dtx35*, *dtx33-1*/*dtx35*, and *dtx33-2*/*dtx35* mutant lines. Although the chloride currents of the three single mutants were moderately reduced, the channel activities in the two double mutants were greatly reduced (Fig. 6*C*). The mean current density recorded from the vacuoles of these two double mutants was −0.5 pA compared with 3 pA in the control at −160 mV (Fig. 6*D*). The result indicated that DTX33 and DTX35 are major channels that additively contribute to voltage-dependent inward chloride current in the tonoplast.

We also measured the Cl^- content of WT and mutant plants in two treatment groups. In one group, plants grew on the 1/2 Murashige and Skoog (MS) medium (containing 3 mM Cl^-) for 2 wk before their Cl^- contents were measured. In the second group, 2-wk-old plants grown on 1/2 MS medium were transferred to 1/2 MS medium supplemented with 97 mM KCl (with a final Cl^- concentration of 100 mM) for 2 d before measuring Cl^- content in these plants. As shown in Fig. 6*E*, the Cl^- content in the double mutant was slightly lower than that in the WT when grown on medium with 3 mM Cl^-. However, when the plants were transferred to 100 mM Cl^- for 2 d, Cl^- accumulation in the double mutants was severely reduced compared with that in the WT and single mutants. We also measured the osmolality of plants of the WT, *dtx33-1*/*dtx35*, *dtx33-2*/*dtx35*, *dtx33-1*, *dtx33-2*, and *dtx35*. The osmolality of *dtx33-1*/*dtx35* and *dtx33-2*/*dtx35* was about 10% lower than that of the WT. However, the single mutant of *dtx33* or *dtx35* showed no significant difference from the WT (Fig. S6). These results indicated that lack of *DTX33* and *DTX35* reduced vacuolar Cl^- accumulation and osmolality of plant cells, resulting in lower turgor pressure in double mutants.

DTX33 and DTX35 Function in Root-Hair and Pollen-Tube Elongation. Vacuolar transport of anions is highly relevant to turgor pressure regulation during cell expansion. DTX33 and DTX35 are tonoplast anion channels that may function in turgor regulation of elongating cells. We examined the expression pattern of the two

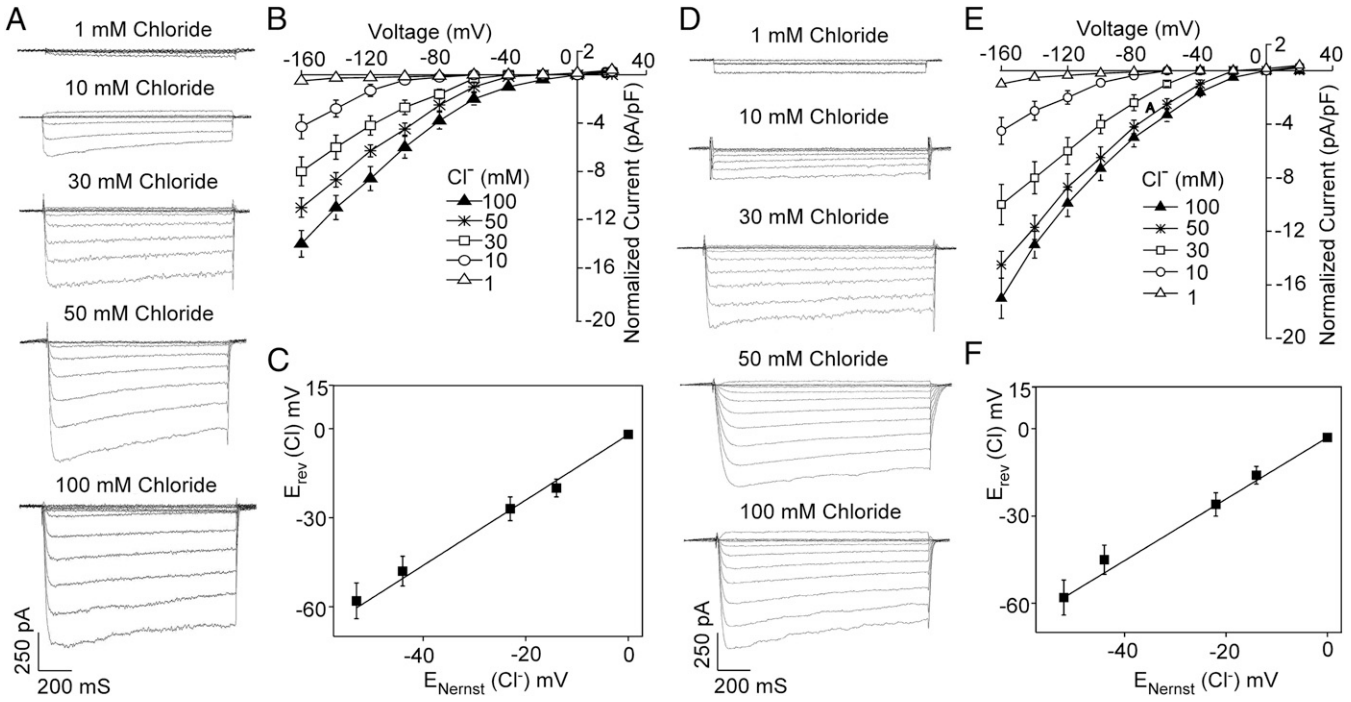

Fig. 4. The DTX33- and DTX35-mediated currents in *N. benthamiana* vacuoles are dependent on chloride concentration. (*A*) The typical whole-vacuole current traces generated by a *DTX33-GFP*–expressing vacuole bathed in solution containing 1, 10, 30, 50, or 100 mM chloride. (*B*) The current–voltage relationship was deduced from recordings of *DTX33-GFP*–expressing vacuoles as in *A*. The data are mean ± SD (n = 15). (*C*) Nernst potentials for Cl^- compared with observed reversal potentials (DTX33) under different chloride concentrations. The linear fit of the data points presents a slope of 1.11 ± 0.12. (*D*) The typical whole-vacuole current traces generated by a *DTX35-GFP*–expressing vacuole bathed in solution containing 1, 10, 30, 50, or 100 mM chloride. (*E*) The current–voltage relationship was deduced from recordings of *DTX35-GFP*–expressing vacuoles as in *D*. The data are mean ± SD (n = 15). (*F*) Nernst potentials for Cl^- compared with observed reversal potentials (DTX35) under different chloride concentrations. The linear fit of the data points presents a slope of 1.04 ± 0.12.

genes encoding these channels and found that they are widely expressed in a variety of plant tissues, including those rapidly elongating cell types, such as root hairs. A root hair is an outgrowth of a root epidermal cell in the mature zone of roots. The development of a root hair starts with cell specification and hair initiation followed by hair elongation, a process also called tip growth (32). We showed that GUS activities driven by either *DTX33* or *DTX35* promoter were strong in root hairs during the early phase of hair elongation (Fig. 7*A* and Fig. S7). Interestingly, when we focused on the same region of root hairs along the developmental process, GUS activity in root hairs reached a peak in 4-d-old plants, when root hairs were in rapid growth phase; then, it decreased and eventually became undetectable when root hairs stopped elongation in 14-d-old plants (Fig. 7 *A*–*C*). This unique pattern of expression suggested that DTX33 and DTX35 may play a role in root-hair elongation, a polarized cell growth that is known to be driven by turgor pressure. We then analyzed the root-hair phenotype of the mutants lacking expression of each of the genes or both of them. We found that the single mutants and two double mutants exhibited shorter root hairs during early growth phase when the seedlings were 4 d old (fourth day after germination) (Fig. 7 *D* and *E*). When we examined the same region of the roots from these plants on the seventh day, we found that root hairs of the single mutants continued to grow and eventually reached similar lengths to those from the WT, but the double mutant still displayed shorter root hairs (Fig. 7 *D* and *F*). Root hairs of all plants were up to the same length when the plants were 14 d old (Fig. 7 *D* and *G*). The delayed root-hair elongation at the early stage precisely matched the expression pattern of the two genes encoding the two tonoplast channels, suggesting that DTX33 and DTX35 function in turgor regulation essential for root-hair growth. The fact that mutant root hairs eventually reached the same length as the WT suggested presence of other unknown channels responsible for supplementing similar function, especially in the later stage of root-hair development.

In addition to the function in root-hair elongation, the *DTX35* was previously shown to play a role in reproduction (33). We also observed lower fertility in the *dtx35* single mutant (Fig. S8*A*). This phenotype prompted us to examine further why the mutant showed a fertility defect by checking the detailed expression pattern of *DTX35*. The *DTX35* promoter–*GUS* reporter was strongly expressed in pollen grains and pollen tubes (Fig. S8*B*), whereas the *DTX33* promoter–*GUS* was not. When we analyzed pollen germination and pollen-tube growth in vitro, we found that pollen tubes from the *dtx35* mutant were significantly shorter compared with those of the WT (Fig. S8 *C*–*E*), but the germination rate of *dtx35* pollen grains was normal. Because turgor pressure is the driving force for pollen-tube elongation as well as root-hair growth, these results suggest that DTX35 and DTX33 work together in root-hair elongation, but DTX35 (not DTX33) plays a role during pollen-tube growth.

The *dtx33/dtx35* Mutant Is Impaired in Stomatal Opening and Becomes More Tolerant to Drought. In addition to expression in root hairs, both DTX33 and DTX35 were also strongly expressed in guard cells (Fig. 2 *C*, *c* and *D*, *c*) that also experience rapid turgor changes during stomatal movements. It is thus plausible that DTX33 and DTX35 may also be involved in the control of stomatal opening that requires turgor-driven expansion of the two guard cells. To test this hypothesis, we measured the rate of water loss from rosette leaves of the WT and various mutants at 23 °C with 60% humidity under light. We found that detached leaves from both double-mutant plants, *dtx33-1*/*dtx35* and *dtx33-2*/*dtx35*, lost water more slowly than those of WT plants and single mutants (Fig. 8*A* and Fig. S9*A*). In the 4-h duration, detached leaves of double mutants (*dtx33-1*/*dtx35* and *dtx33-2*/*dtx35*) lost 35% of fresh

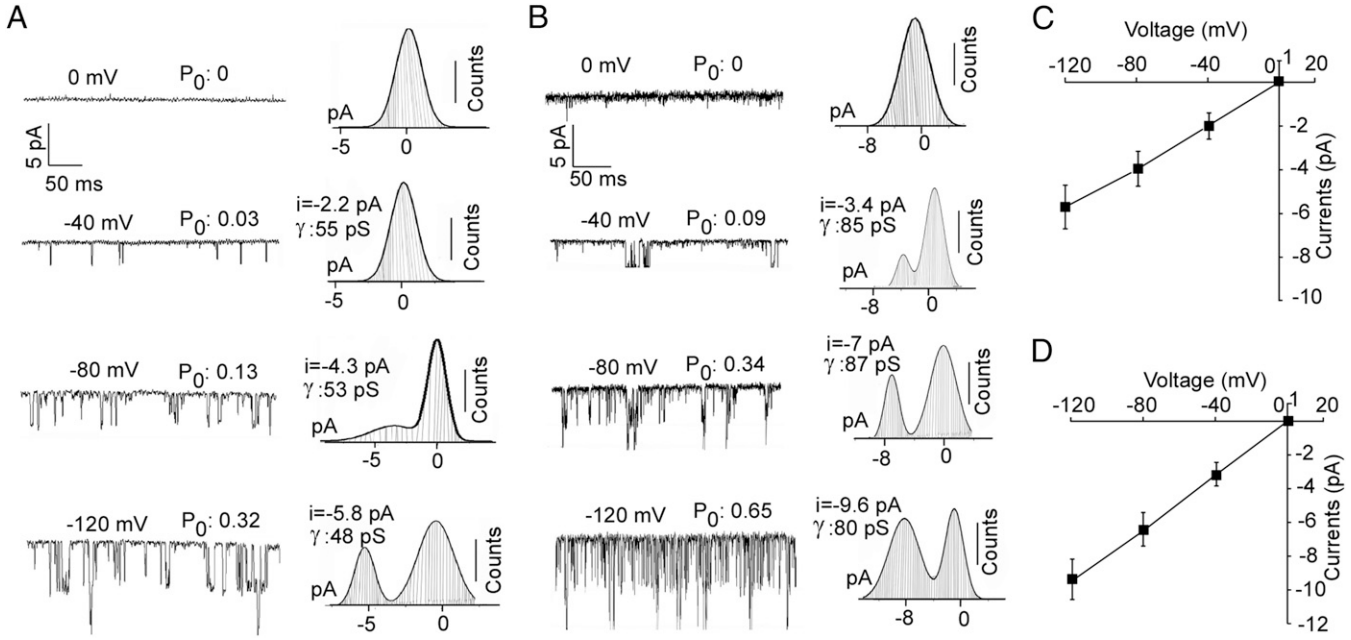

Fig. 5. The DTX33- and DTX35-mediated currents in *N. benthamiana* vacuoles are voltage-sensitive. (*A*) The Po of *DTX33-GFP*–expressing vacuole single channels in excised outside-out patches at different voltages. (*Left*) Representative current traces and (*Right*) corresponding amplitude histograms recorded at (*Left*) membrane potentials of 0, −40, −80, or −120 mV. The conductance (γ) was calculated as the current to voltage ratio. (*B*) The Po of *DTX35-GFP*–expressing vacuole single channels in excised outside-out patches at different voltages. (*Left*) Representative current traces and (*Right*) corresponding amplitude histograms recorded at (*Left*) membrane potentials of 0, −40, −80, or −120 mV. The conductance (γ) was calculated as the current to voltage ratio. (*C*) Current–voltage relationship of *DTX33-GFP*–expressing vacuole recordings from eight excised outside-out patches under various membrane potentials. Data are mean ± SD. (*D*) Current–voltage relationship of *DTX35-GFP*–expressing vacuole recordings from eight excised outside-out patches under various membrane potentials. Data are mean ± SD.

weight and the single mutants (*dtx33-1* and *dtx35*) lost about 50% compared with WT leaves, which lost about 60% fresh weight (Fig. 8*A*). We further measured stomatal conductance of leaves on intact plants that were grown under a normal light–dark cycle. When the plants from the dark period were exposed to the light (130 μmol m^{-2} s^{-1}) to induce stomatal opening, stomatal conductance was lower in the mutants, especially *dtx33-1*/*dtx35* and *dtx33-2*/*dtx35* double mutants, compared with the WT (Fig. 8*B*). Stomatal conductance in the single mutants was again slightly lower than in the WT, indicating that both channels contribute to cell turgor in an additive manner. When plants were transferred to the dark, the WT and mutants showed similar rate of stomatal closing.

We also carried out experiments with epidermal strips in different buffers to compare mutants with WT plants in stomatal movements. We placed the leaves of the WT and mutants in the stomatal opening buffer containing 5 mM Cl^- and incubated them in the dark. Stomata of dark-incubated leaves were closed, and no difference was found between the WT and mutants. When exposed to light for 3 h, peeled epidermal strips of *dtx33-1*/*dtx35* and *dtx33-2*/*dtx35* exhibited smaller stomatal aperture than the WT. Interestingly, when exposed to light in the stomatal opening buffer with an increased Cl^- concentration (30 mM) for 3 h, WT leaves showed larger stomatal aperture compared with those incubated in 5 mM Cl^-. However, the double mutants showed smaller stomatal aperture in both cases, and no difference was observed between samples in 5 or 30 mM Cl^- (Fig. 8*C*). This result suggests that Cl^- accumulation into the vacuole contributes to turgor regulation and that lack of *DTX33* and *DTX35* reduced Cl^- influx, thereby lowering the driving force for stomatal opening. Furthermore, ABA-induced stomatal closing, like dark-induced closing, was not altered in the double mutants compared with the WT.

To examine whether the difference in stomatal conductance between the WT and the mutants affected their water-holding efficiency under physiological conditions, we tested drought tolerance in the WT, two double mutants (*dtx33-1*/*dtx35* and *dtx33-2*/*dtx35*), and two complementation lines (*dtx33-1*/*dtx35* complemented by *35S-DTX33* and *dtx33-1*/*dtx35* complemented by *35S-DTX35*). After withholding water for 10 d from 8-wk-old plants under short-day 8-/16-h greenhouse conditions, we found that double-mutant plants wilted more slowly than the WT and complementation lines (Fig. 8*D*). Prolonged drought treatment revealed more clear difference between the WT and the double mutant (Fig. S9*B*). Taken together, these results indicate that DTX33 and DTX35 play a significant role in the control of stomatal opening, thereby contributing to the gas exchange function of the plants.

Discussion

Plant cell growth and stature are determined by turgor pressure largely produced by concentrated solutes in the vacuolar lumen. A large number of transport proteins in the tonoplast control the trafficking of solutes in and out of the vacuole, providing a molecular network that regulates turgor pressure. To understand the molecular mechanism underlying cell growth and turgor regulation, it is essential that the function of these transporters be dissected. Here, we report identification of two tonoplast MATE-type proteins that function as CLCs essential for turgor regulation in plants.

Organic compounds, including a number of therapeutic drugs, have been shown to be substrates of MATE transporters in bacteria and animals (15, 34, 35). The MATE/DTX proteins in plants constitute a superfamily, and some of them have been shown to transport organic acids or secondary metabolites (16–22, 29, 36). For example, MATE proteins play a role in aluminum tolerance by mediating citric acid efflux from root cells (29, 37–40) to chelate Al^{3+} (29, 35–39). So far, however, none of the MATE proteins from any organism have been shown to transport inorganic anions. Finding DTX33 and DTX35 as

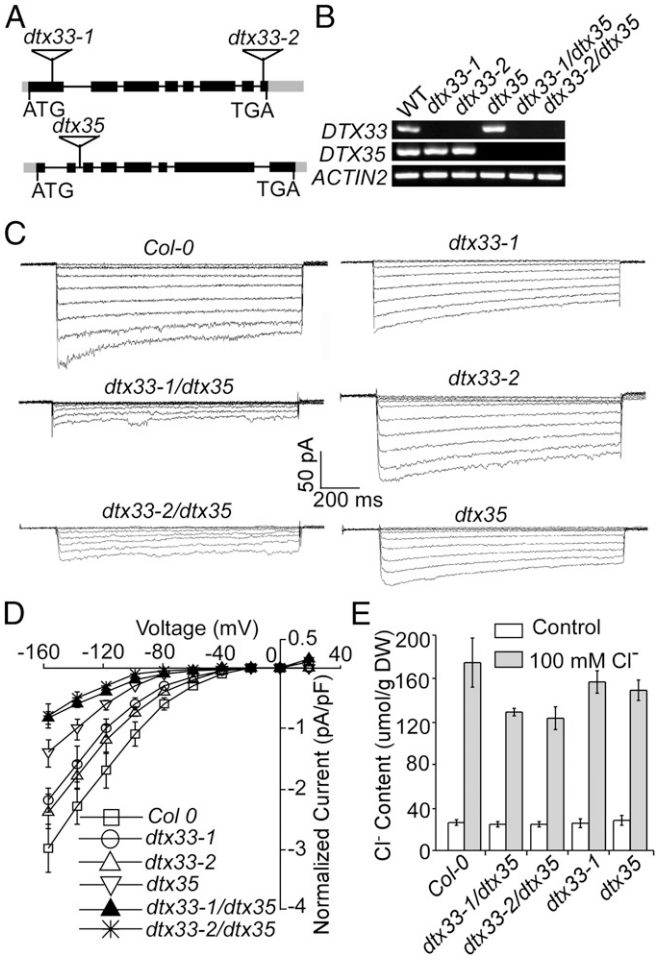

Fig. 6. Whole-vacuole Cl^- currents are impaired in vacuoles isolated from mutant plants lacking *dtx33* and *dtx35*. (*A*) Schematic map of the *dtx33* and *dtx35* insertion mutants used in this study. (*B*) RT-PCR analysis of mRNA levels in the WT; *dtx33-1*, *dtx33-2*, and *dtx35* single mutants; and *dtx33-1/dtx35* and *dtx33-2/dtx35* double mutants. The total RNA samples were extracted from *Arabidopsis* rosette leaves of 4-wk-old plants in soil. (*C*) Representative traces of the currents recorded in whole-vacuole configuration from *Col-0*, two double mutants (*dtx33-1/dtx35* and *dtx33-2/dtx35*), and three single mutants (*dtx33-1*, *dtx33-2*, and *dtx35*). With a holding potential of 0 mV, currents evoked on 20-mV steps in the voltage range from −160 to +20 mV. (*D*) Corresponding *I-V* curves (*Col-0*, $n = 21$; *dtx33-1*, $n = 15$; *dtx33-2*, $n = 13$; *dtx35*, $n = 17$; *dtx33-1/dtx35*, $n = 14$; *dtx33-2/dtx35*, $n = 12$). Steady-state currents were determined by averaging the last 100 ms of each current trace for inward currents. Data present mean ± SD. (*E*) Cl^- contents in the plants of *Col-0*, *dtx33-1/dtx35*, *dtx33-2/dtx35*, *dtx33-1*, and *dtx35*. The white bars denote plants grown under 3 mM Cl^-, and the gray bars indicate plants grown under 3 mM Cl^- for 2 wk and transferred to 100 mM Cl^- for 2 d before the whole plants were harvested and used for measuring Cl^- contents. Five independent experiments were carried out, and data represent mean ± SD.

CLCs in this study is significant, because it breaks the dogma that DTX/MATE proteins are transporters of organic compounds. Our work thus expands the diversity of substrates for plant MATE transporters, extending the function of this large family of transporters to basic turgor regulation in addition to detoxification of secondary metabolites and heavy metals as originally proposed (16). This finding also adds a family to the list of anion/CLCs that includes the previously known voltage-gated CLC family, aluminum-activated malate transporters (ALMTs), and slow-type anion channels (SLACs).

In the context of multiple anion channel families, it will be particularly important to sort out the physiological functions of individual channel family. The CLC family proteins are conserved in species from bacteria to human and function as Cl^- channels or Cl^-/H^+ antiporters (41). Based on several studies on the two model plants *Arabidopsis* and rice, members of the CLC family have been proposed to function as anion channels/transporters. Four of seven CLC members in *Arabidopsis* are localized to tonoplast (9). Combining electrophysiological and genetic approaches, De Angeli et al. (30) showed that AtClCa functions as an NO_3^-/H^+ exchanger responsible specifically for nitrate transport into the vacuole and that it is involved in nitrate homeostasis between cytoplasm and vacuole (9, 42). The CLCc protein can transport both nitrate and chloride and is involved in chloride homeostasis in guard cells (43, 44). The ALMTs were first identified in wheat (TaALMT1) and rape seed (45, 46), where these ALMT proteins mediate malate efflux to detoxify soil-borne Al^{3+} by chelating the toxic cation (47). In *Arabidopsis*, *ALMT* genes are categorized into three clades according to sequence comparison (47). The first clade has the highest homology to TaALMT1, and within this group, AtALMT1 is crucial for aluminum tolerance (48). It is shown that genes in the second clade, such as AtALMT6 and AtALMT9, give rise to vacuolar anion channels (28, 49), whereas those of the third clade, including QUAC1, encode plasma membrane R-type channels found in various cell types, including guard cells (50, 51). The SLACs are first identified from *Arabidopsis* and show weak homology to the tellurite resistance multidrug transporter TehA from *Haemophilus influenzae* and the malate transporter Mae1 from fission yeast (52). Studies place SLAC1 family channels as key regulators of guard cell turgor and thus, stomatal movements in response to various signals, including high CO_2 and ABA (53–55). Both SLAC1 and SLAH3 are localized in the plasma membrane of guard cells and mediate the efflux of anions (chloride and nitrate) to regulate stomatal closure (56–59).

Identifying the function of DTX33 and DTX35 as tonoplast chloride/anion channels expands the repertoire of anion channels in plant cells in general and vacuolar anion channels in particular. What is the specific function of DTX33 and DTX35 (and possibly, other DTX members in the same category) in vacuolar turgor regulation? To date, CLCa, CLCc, ALMT9, and ALMT6 are known to function as tonoplast transporters/channels that may function in a similar way as DTX33 and DTX35, in that they all mediate anion influx into the vacuole. Although CLCa specifically transports NO_3^-, it functions as $2NO_3^-/1H^+$ exchanger (30). ALMT6 and ALMT9 are anion channels that are permeable to various anions, including Cl^- and malate. Studies indicate that both ALMT6 and ALMT9 function as anion channels for turgor regulation in guard cells controlling stomatal opening. The ALMT6 protein transports malate and fumarate, which are present in guard cells in large quantities (49). The ALMT9 protein is a malate-activated CLC in guard cells (26). Under certain conditions, CLCa and its homologs may also play a role in stomatal movement (44, 60). Our study here shows that DTX33 and DTX35, although structurally unrelated to ALMTs or CLCs, are both CLCs that function in turgor regulation in guard cells. However, DTX33 and DTX35 have specific properties that are different from known channels. Unlike some CLC family members that function as anion H^+ antiporters, the measured reversal potentials of DTX33 and DTX35 are in total agreement with the theoretical Nernst potentials under different ionic conditions (Fig. 4 *C* and *F*), indicating that DTX33 and DTX35 function as ion channels. Because homologs of DTX33 and DTX35 are present in many plants (Figs. S10 and S11), we believe that DTX channels are generally important for turgor regulation in the plant kingdom. We noted that the activity of these channels can be regulated by vacuolar pH changes, reminiscent of the pH dependence observed with ALMT6 (49) (Fig. S12). Meanwhile, compared with ALMT family members, DTX33 and DTX35 exhibit the highest selectivity for Cl^- over

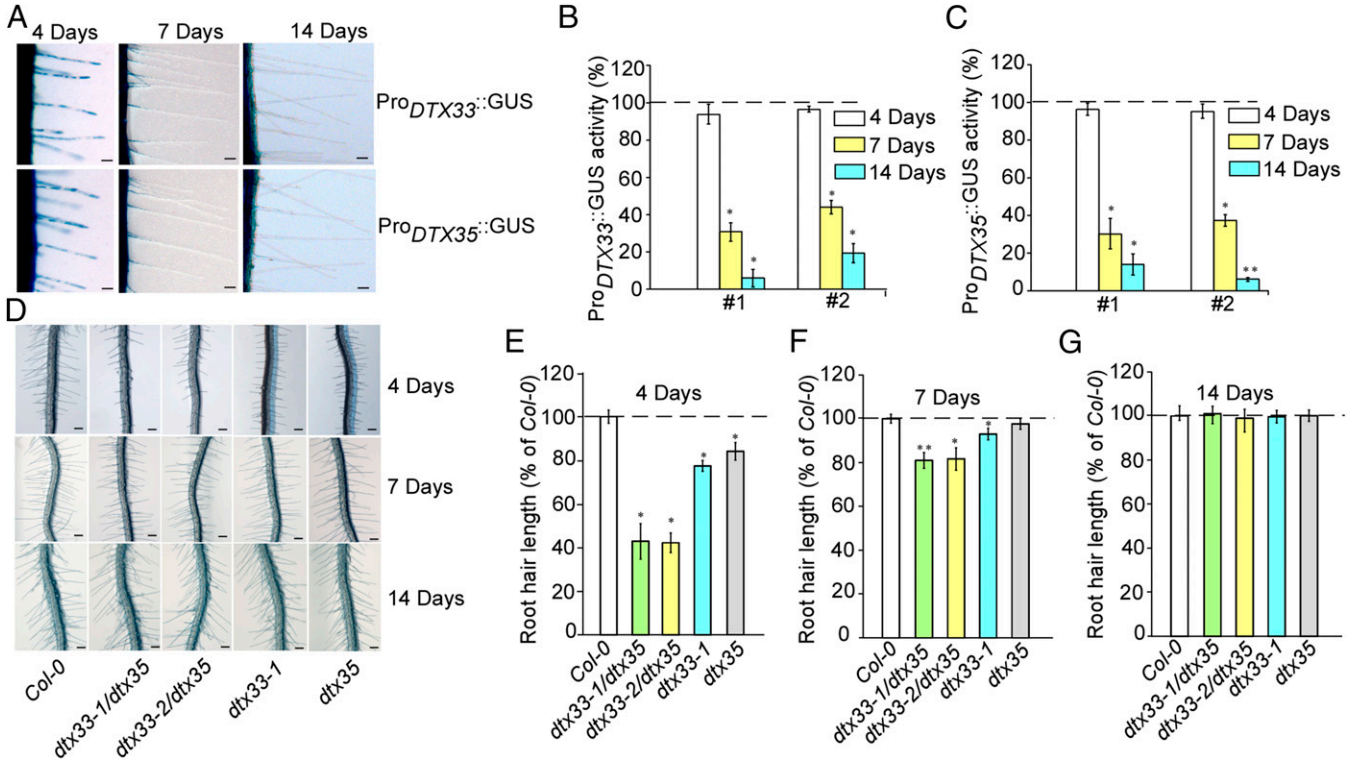

Fig. 7. The double mutants showed delayed root-hair elongation. (*A*) GUS staining shows the expression of *DTX33* and *DTX35* in root hairs at different developmental stages. (Scale bars: 4 d, 50 μm; 7 and 14 d, 0.1 mm.) (*B* and *C*) Quantification of GUS activity in the root hairs of transgenic *Arabidopsis* plants containing the *DTX33* (*B*) and *DTX35* (*C*) promoter–GUS construct. ImageJ software was used to quantify the GUS signals in the root hairs of two transgenic lines (lines 1 and 2) at different ages. Three plants from each line were used for the analysis in one experiment. The experiment was repeated three times with similar results. Data are means ± SEM, and Student's *t* test was used to identify significant differences at the $P < 0.05$ or 0.01 level. $*P < 0.05$; $**P < 0.01$. (*D*) Images of roots from 4-d-old *Col-0*, *dtx33-1/dtx35*, *dtx33-2/dtx35*, *dtx-1*, and *dtx35*. (Scale bars: 4 d, 0.25 mm; 7 d, 0.3 mm; 14 d, 0.2 mm.) (*E*–*G*) Comparison of the root-hair lengths of *Col-0* and mutant plants at 4, 7, and 14 d. Mutant lines were *dtx33-1/dtx35*, *dtx33-2/dtx35*, *dtx33-1*, and *dtx35*. The bar graphs show average lengths of 400 (*Col-0*), 232 (*dtx33-1/dtx35*), 201 (*dtx33-2/dtx35*), 180 (*dtx33-1*), and 355 (*dtx35*) root hairs for 4-d-old plants (*E*); 280 (*Col-0*), 165 (*dtx33-1/dtx35*), 186 (*dtx33-2/dtx35*), 158 (*dtx33-1*), and 213 (*dtx35*) root hairs for 7-d-old plants (*F*); and 210 (*Col-0*), 155 (*dtx33-1/dtx35*), 167 (*dtx33-2/dtx35*), 138 (*dtx33-1*), and 198 (*dtx35*) for 14-d-old plants (*G*). Data are means ± SEM, and Student's *t* test was used to identify significant differences at the $P < 0.05$ or $P < 0.01$ level. $*P < 0.05$; $**P < 0.01$.

other anions in plants (Fig. 3 *D* and *E*) but are not significantly permeable to organic acids, such as citric acid and malate. Interestingly, mutations in ALMT or DTX channels all lead to defects in stomatal opening to a certain degree, suggesting that these channels function in turgor regulation of guard cells but not in a redundant fashion. It will be interesting to dissect their individual contributions to guard cell physiology by producing stacking mutants combining the mutations and comparing with each individual mutant. Without doubt, a complex battery of channels in the tonoplast works together to fine-tune cell turgor, so that plant cells can adapt to constantly changing environments.

In addition to guard cells, the DTX channels are also highly expressed in root hairs, especially in the early stage of root-hair development. Indeed, these DTX channels participate in root-hair elongation at least during the early phase. Through this work, we realized that other channels/transporters are also involved in the control of root-hair turgor pressure, because disruption of both DTX channels failed to affect the length of mature root hairs. Identifying the other players in this process will help clarify the individual contributions of multiple channels/transporters to turgor regulation in root hairs, a model system for studying polarized cell elongation.

A wide-spreading pattern of expression of *DTX33* and *DTX35* warrants additional analysis of their function in other cell types in addition to guard cells and root hairs. In this regard, an earlier study shows that lack of *DTX35* affects pollen development and flavonoid content in flowers, leading to the hypothesis that DTX35, like TT12, may be a flavonoid transporter (33). We also observed fertility defects in the *dtx35* mutant. Furthermore, when pollen grains were cultured and germinated in vitro, pollen tubes of *dtx35* mutant grew more slowly compared those of the WT (Fig. S8). We, therefore, hypothesize that the fertility defect in the mutant may have derived from reduced pollen tube growth, which as in the case of root-hair growth, also requires proper turgor pressure to drive cell elongation. To our knowledge, function of tonoplast channels in pollen-tube growth has not been previously reported, and additional analysis along this line will shed light on the contribution of vacuolar transport in polar growth. It will not be surprising if these channels are found to contribute to turgor regulation in many other cell types and under various environmental conditions. Furthermore, finding the two DTX/MATE transporters as CLCs raises the possibility that other MATE proteins may also function as ion channels, which should be addressed in future studies.

Materials and Methods

Plant Materials and Growth Conditions. All *Arabidopsis* plants were grown in soil under greenhouse conditions (22 °C; 16-/8-h light–dark cycle for long day; 8-/16-h light–dark cycle for short day; 80–100 μmol m^{-2} s^{-1} light intensity) or on 1/2 MS medium containing 0.5% sucrose and 0.8% agar in the growth chamber (22 °C/18 °C; 16-/8-h light–dark cycle; 80 μmol m^{-2} s^{-1} light intensity). Mutant seeds were obtained from the *Arabidopsis* Biological Resource Center (*dtx33-1* as SALK_084030, *dtx33-2* as SALK_131275, and *dtx35* as SALK_104224).

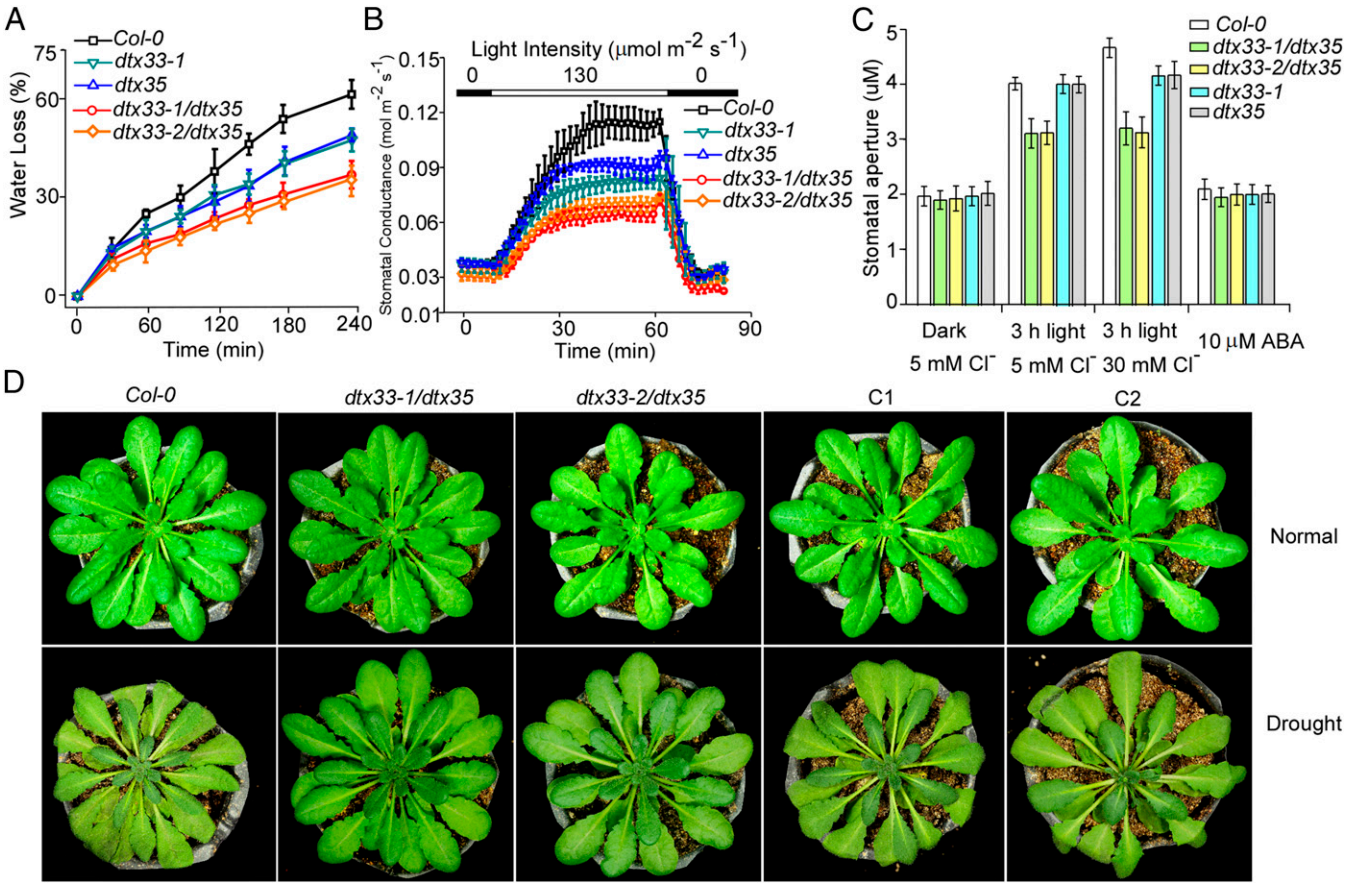

Fig. 8. The *dtx33* and *dtx35* mutants are impaired in stomatal opening and show altered drought tolerance. (*A*) Time course of water loss from the detached leaves of 4-wk-old *Col-0*, *dtx33-1/dtx35*, *dtx33-2/dtx35*, *dtx33-1*, and *dtx35* plants. Water loss rate is shown as a percentage of the initial fresh weight at indicated intervals. Three independent experiments were carried out, and three plants were used for each experiment. The mean values of three measurements are shown with error bars (± SD). (*B*) Time course of stomatal conductance of *Col-0*, *dtx33-1/dtx35*, *dtx33-2/dtx35*, *dtx33-1*, and *dtx35* plants during light-induced opening. Plants were preincubated under dark and 400 ppm CO_2; 130 μmol m^{-2} s^{-1} light was given, and transpiration rate was recorded for 50 min and then, returned to dark. The mean values of three measurements are shown with error bars (± SD). (*C*) Stomotal aperture of *Col-0*, *dtx33-1/dtx35*, *dtx33-2/dtx35*, *dtx33-1*, and *dtx35* plants in the presence of 5 or 30 mM Cl^- or 10 μM ABA. Three independent experiments were carried out, and about 50 guard cells were measured for each sample in each experiment. Data are means ± SD. (*D*) Photographs of 8-wk-old short-day plants of *Col-0* and *dtx33-1/dtx35* and *dtx33-2/dtx35* double mutants and complemented lines transformed with *35S-DTX33* (C1) or *35S-DTX35* (C2) grown under (*Upper*) normal conditions or (*Lower*) 10 d after withholding water.

Subcellular Localization of DTX33::GFP and DTX35::GFP Fusion Proteins. pCambia1302-*35S-DTX33::GFP*, pCambia1302-*35S-DTX35::GFP*, and pCambia1302-*35S-GFP* constructs were introduced into *Arabidopsis* suspension culture or *Arabidopsis* mesophyll protoplasts by the PEG-mediated transfection procedure (24). Protoplast cells were resuspended in 1 mL W5 wash solution (containing 154 mM NaCl, 125 mM $CaCl_2$, 5 mM $MgCl_2$, 2 mM MES adjusted to pH 5.7 with KOH) and cultured for 18 h in the dark at room temperature. Confocal images were captured using Zeiss Live 5 equipment. The fluorescence signals were excited at 488 nm for GFP. The primers used are summarized in Table S3.

GUS Activity Assay. GUS activity was detected by histochemical staining of tissues as previously described (61). The GUS-stained plants were examined under the microscope (Zeiss Stemi SV11), and digital images were captured using the Zeiss Axio Vision software.

Ectopic Expression of *DTX33-GFP* and *DTX35-GFP* in *N. benthamiana* and Isolation of Mesophyll Vacuoles. The *DTX33* and *DTX35* cDNAs were cloned into the pCambia1302 vector and transformed into agrobacterium GV3101 for infiltration of *N. benthamiana* leaves (62). Three days after infiltration, the mesophyll protoplasts from transformed tobacco leaves were released by an enzymatic digestion, and vacuoles were further released from the protoplasts as described previously (26).

Patch-Clamp Recordings on Mesophyll Vacuoles. Patch-clamp experiments on mesophyll vacuoles were performed in whole-vacuole and excised cytosolic side-out configurations as described previously (27, 63). Additional details are described in *SI Materials and Methods*.

Cl^- Content Measurement. Cl^- contents were determined by a modified silver titration method that has been described previously (64).

Observation of Root-Hair Growth Phenotypes. Root-hair length was measured as described (65) with modifications. Portion of the root with uniform root hairs was digitally photographed with a stereomicroscope (MZ FLIII; Leica). The length of 10 consecutive hairs protruding perpendicularly from each side of the root for a total of 20 hairs from both sides of the root was calculated using LAS software, version 2.8.1 (Leica).

Measurement of Stomatal Conductance and Stomatal Aperture. To analyze stomatal responses to light–dark transitions, we chose mature nonsenescent leaves of 6-wk-old plants for gas exchange experiments using a Li-6400 IR (IRGA) Gas Exchange Analyzer. The experiments were conducted under 22 °C and 60% humidity conditions as described previously (26). Stomatal aperture measurements are described in *SI Materials and Methods*.

ACKNOWLEDGMENTS. This work was supported by National Natural Science Foundation of China Grants 31570265 (to H.Z.), 31270303 (to F.-G.Z.), and 31270297 (to L.L.); National Key Research and Development Program of China Grant 2016YFD0300102-3 (to L.L.); and a grant from the National Science Foundation (to S.L.).

1. Geitmann A, Ortega JK (2009) Mechanics and modeling of plant cell growth. *Trends Plant Sci* 14(9):467–478.
2. Hamant O, Traas J (2010) The mechanics behind plant development. *New Phytol* 185(2):369–385.
3. Robinson S, et al. (2013) Mechanical control of morphogenesis at the shoot apex. *J Exp Bot* 64(15):4729–4744.
4. Peters WS, Tomos AD (1996) The history of tissue tension. *Ann Bot (Lond)* 77(6): 657–665.
5. Echeverria E, Burns JK (1989) Vacuolar Acid hydrolysis as a physiological mechanism for sucrose breakdown. *Plant Physiol* 90(2):530–533.
6. Sun-Wada GH, Wada Y (2015) Role of vacuolar-type proton ATPase in signal transduction. *Biochim Biophys Acta* 1847(10):1166–1172.
7. Klein M, Burla B, Martinoia E (2006) The multidrug resistance-associated protein (MRP/ABCC) subfamily of ATP-binding cassette transporters in plants. *FEBS Lett* 580(4):1112–1122.
8. Hwang JU, et al. (2016) Plant ABC transporters enable many unique aspects of a terrestrial plant's lifestyle. *Mol Plant* 9(3):338–355.
9. Zifarelli G, Pusch M (2010) CLC transport proteins in plants. *FEBS Lett* 584(10): 2122–2127.
10. Apse MP, Aharon GS, Snedden WA, Blumwald E (1999) Salt tolerance conferred by overexpression of a vacuolar Na+/H+ antiport in Arabidopsis. *Science* 285(5431): 1256–1258.
11. Gobert A, Isayenkov S, Voelker C, Czempinski K, Maathuis FJ (2007) The two-pore channel TPK1 gene encodes the vacuolar K+ conductance and plays a role in K+ homeostasis. *Proc Natl Acad Sci USA* 104(25):10726–10731.
12. Islam MM, et al. (2010) Roles of AtTPC1, vacuolar two pore channel 1, in *Arabidopsis* stomatal closure. *Plant Cell Physiol* 51(2):302–311.
13. Martinoia E, Meyer S, De Angeli A, Nagy R (2012) Vacuolar transporters in their physiological context. *Annu Rev Plant Biol* 63:183–213.
14. Maurel C, et al. (2015) Aquaporins in plants. *Physiol Rev* 95(4):1321–1358.
15. Omote H, Hiasa M, Matsumoto T, Otsuka M, Moriyama Y (2006) The MATE proteins as fundamental transporters of metabolic and xenobiotic organic cations. *Trends Pharmacol Sci* 27(11):587–593.
16. Li L, He Z, Pandey GK, Tsuchiya T, Luan S (2002) Functional cloning and characterization of a plant efflux carrier for multidrug and heavy metal detoxification. *J Biol Chem* 277(7):5360–5368.
17. Marinova K, et al. (2007) The Arabidopsis MATE transporter TT12 acts as a vacuolar flavonoid/H+ -antiporter active in proanthocyanidin-accumulating cells of the seed coat. *Plant Cell* 19(6):2023–2038.
18. Durrett TP, Gassmann W, Rogers EE (2007) The FRD3-mediated efflux of citrate into the root vasculature is necessary for efficient iron translocation. *Plant Physiol* 144(1): 197–205.
19. Nawrath C, Heck S, Parinthawong N, Métraux JP (2002) EDS5, an essential component of salicylic acid-dependent signaling for disease resistance in *Arabidopsis*, is a member of the MATE transporter family. *Plant Cell* 14(1):275–286.
20. Serrano M, et al. (2013) Export of salicylic acid from the chloroplast requires the multidrug and toxin extrusion-like transporter EDS5. *Plant Physiol* 162(4): 1815–1821.
21. Zhang H, et al. (2014) A DTX/MATE-type transporter facilitates abscisic acid efflux and modulates ABA sensitivity and drought tolerance in *Arabidopsis*. *Mol Plant* 7(10): 1522–1532.
22. Dobritzsch M, et al. (2016) MATE transporter-dependent export of hydroxycinnamic acid amides. *Plant Cell* 28(2):583–596.
23. Jaquinod M, et al. (2007) A proteomics dissection of *Arabidopsis thaliana* vacuoles isolated from cell culture. *Mol Cell Proteomics* 6(3):394–412.
24. Miao Y, Jiang L (2007) Transient expression of fluorescent fusion proteins in protoplasts of suspension cultured cells. *Nat Protoc* 2(10):2348–2353.
25. Latz A, et al. (2007) TPK1, a Ca(2+)-regulated *Arabidopsis* vacuole two-pore K(+) channel is activated by 14-3-3 proteins. *Plant J* 52(3):449–459.
26. De Angeli A, Zhang J, Meyer S, Martinoia E (2013) AtALMT9 is a malate-activated vacuolar chloride channel required for stomatal opening in *Arabidopsis*. *Nat Commun* 4:1804–1814.
27. Liu J, et al. (2015) A vacuolar phosphate transporter essential for phosphate homeostasis in *Arabidopsis*. *Proc Natl Acad Sci USA* 112(47):E6571–E6578.
28. Kovermann P, et al. (2007) The *Arabidopsis* vacuolar malate channel is a member of the ALMT family. *Plant J* 52(6):1169–1180.
29. Maron LG, et al. (2010) Two functionally distinct members of the MATE (multi-drug and toxic compound extrusion) family of transporters potentially underlie two major aluminum tolerance QTLs in maize. *Plant J* 61(5):728–740.
30. De Angeli A, et al. (2006) The nitrate/proton antiporter AtCLCa mediates nitrate accumulation in plant vacuoles. *Nature* 442(7105):939–942.
31. Bertl A, Slayman CL (1992) Complex modulation of cation channels in the tonoplast and plasma membrane of Saccharomyces cerevisiae: Single-channel studies. *J Exp Biol* 172:271–287.
32. Won SK, et al. (2009) Cis-element- and transcriptome-based screening of root hair-specific genes and their functional characterization in Arabidopsis. *Plant Physiol* 150(3):1459–1473.
33. Thompson EP, Wilkins C, Demidchik V, Davies JM, Glover BJ (2010) An *Arabidopsis* flavonoid transporter is required for anther dehiscence and pollen development. *J Exp Bot* 61(2):439–451.
34. Kuroda T, Tsuchiya T (2009) Multidrug efflux transporters in the MATE family. *Biochim Biophys Acta* 1794(5):763–768.
35. Lu M (2016) Structures of multidrug and toxic compound extrusion transporters and their mechanistic implications. *Channels (Austin)* 10(2):88–100.
36. Diener AC, Gaxiola RA, Fink GR (2001) *Arabidopsis* ALF5, a multidrug efflux transporter gene family member, confers resistance to toxins. *Plant Cell* 13(7): 1625–1638.
37. Furukawa J, et al. (2007) An aluminum-activated citrate transporter in barley. *Plant Cell Physiol* 48(8):1081–1091.
38. Magalhaes JV, et al. (2007) A gene in the multidrug and toxic compound extrusion (MATE) family confers aluminum tolerance in sorghum. *Nat Genet* 39(9): 1156–1161.
39. Yokosho K, Yamaji N, Ma JF (2011) An Al-inducible MATE gene is involved in external detoxification of Al in rice. *Plant J* 68(6):1061–1069.
40. Yokosho K, Yamaji N, Fujii-Kashino M, Ma JF (2016) Functional analysis of a MATE gene OsFRDL2 revealed its involvement in Al-induced secretion of citrate, but a lower contribution to Al tolerance in rice. *Plant Cell Physiol* 57(5):976–985.
41. Mindell JA, Maduke M (2001) ClC chloride channels. *Genome Biol* 2(2):REVIEWS3003.
42. De Angeli A, et al. (2009) Review. CLC-mediated anion transport in plant cells. *Philos Trans R Soc Lond B Biol Sci* 364(1514):195–201.
43. Harada H, Kuromori T, Hirayama T, Shinozaki K, Leigh RA (2004) Quantitative trait loci analysis of nitrate storage in *Arabidopsis* leading to an investigation of the contribution of the anion channel gene, AtCLC-c, to variation in nitrate levels. *J Exp Bot* 55(405):2005–2014.
44. Jossier M, et al. (2010) The *Arabidopsis* vacuolar anion transporter, AtCLCc, is involved in the regulation of stomatal movements and contributes to salt tolerance. *Plant J* 64(4):563–576.
45. Sasaki T, et al. (2004) A wheat gene encoding an aluminum-activated malate transporter. *Plant J* 37(5):645–653.
46. Ligaba A, Katsuhara M, Ryan PR, Shibasaka M, Matsumoto H (2006) The BnALMT1 and BnALMT2 genes from rape encode aluminum-activated malate transporters that enhance the aluminum resistance of plant cells. *Plant Physiol* 142(3): 1294–1303.
47. Delhaize E, Gruber BD, Ryan PR (2007) The roles of organic anion permeases in aluminium resistance and mineral nutrition. *FEBS Lett* 581(12):2255–2262.
48. Hoekenga OA, et al. (2006) AtALMT1, which encodes a malate transporter, is identified as one of several genes critical for aluminum tolerance in *Arabidopsis*. *Proc Natl Acad Sci USA* 103(25):9738–9743.
49. Meyer S, et al. (2011) Malate transport by the vacuolar AtALMT6 channel in guard cells is subject to multiple regulation. *Plant J* 67(2):247–257.
50. Hedrich R (2012) Ion channels in plants. *Physiol Rev* 92(4):1777–1811.
51. Mumm P, et al. (2013) C-terminus-mediated voltage gating of *Arabidopsis* guard cell anion channel QUAC1. *Mol Plant* 6(5):1550–1563.
52. Chen YH, et al. (2010) Homologue structure of the SLAC1 anion channel for closing stomata in leaves. *Nature* 467(7319):1074–1080.
53. Negi J, et al. (2008) CO2 regulator SLAC1 and its homologues are essential for anion homeostasis in plant cells. *Nature* 452(7186):483–486.
54. Vahisalu T, et al. (2008) SLAC1 is required for plant guard cell S-type anion channel function in stomatal signalling. *Nature* 452(7186):487–491.
55. Geiger D, et al. (2009) Activity of guard cell anion channel SLAC1 is controlled by drought-stress signaling kinase-phosphatase pair. *Proc Natl Acad Sci USA* 106(50): 21425–21430.
56. Geiger D, et al. (2010) Guard cell anion channel SLAC1 is regulated by CDPK protein kinases with distinct Ca2+ affinities. *Proc Natl Acad Sci USA* 107(17):8023–8028.
57. Zheng X, He K, Kleist T, Chen F, Luan S (2015) Anion channel SLAH3 functions in nitrate-dependent alleviation of ammonium toxicity in *Arabidopsis*. *Plant Cell Environ* 38(3):474–486.
58. Lee SC, Lan W, Buchanan BB, Luan S (2009) A protein kinase-phosphatase pair interacts with an ion channel to regulate ABA signaling in plant guard cells. *Proc Natl Acad Sci USA* 106(50):21419–21424.
59. Geiger D, et al. (2011) Stomatal closure by fast abscisic acid signaling is mediated by the guard cell anion channel SLAH3 and the receptor RCAR1. *Sci Signal* 4(173): ra32.
60. Wege S, et al. (2014) Phosphorylation of the vacuolar anion exchanger AtCLCa is required for the stomatal response to abscisic acid. *Sci Signal* 7(333):ra65.
61. Sundaresan V, et al. (1995) Patterns of gene action in plant development revealed by enhancer trap and gene trap transposable elements. *Genes Dev* 9(14): 1797–1810.
62. Yang KY, Liu Y, Zhang S (2001) Activation of a mitogen-activated protein kinase pathway is involved in disease resistance in tobacco. *Proc Natl Acad Sci USA* 98(2): 741–746.
63. Bertl A, et al. (1992) Electrical measurements on endomembranes. *Science* 258(5084): 873–874.
64. Zhang WW, Yang HQ, You SZ, Fan SL, Ran K (2015) MhNCED3, a gene encoding 9-cis-epoxycarotenoid dioxygenase in Malus hupehensis Rehd., enhances plant tolerance to Cl^- stress by reducing Cl^- accumulation. *Plant Physiol Biochem* 89: 85–91.
65. Lee SH, Cho HT (2006) PINOID positively regulates auxin efflux in *Arabidopsis* root hair cells and tobacco cells. *Plant Cell* 18(7):1604–1616.
66. Beyhl D, et al. (2009) The fou2 mutation in the major vacuolar cation channel TPC1 confers tolerance to inhibitory luminal calcium. *Plant J* 58(5):715–723.
67. Ward JM, Schroeder JI (1994) Calcium-activated K^+ channels and calcium-induced calcium release by slow vacuolar ion channels in guard cell vacuoles implicated in the control of stomatal closure. *Plant Cell* 6(5):669–683.